

Fasting-mimicking diet synergizes with ferroptosis against quiescent, chemotherapy-resistant cells

Xiaoxia Liu,^{a,b,c,*} Shaoyong Peng,^{a,c} Guannan Tang,^{a,b} Gaopo Xu,^{a,b} Yumo Xie,^{a,b} Dingcheng Shen,^{a,b} Mingxuan Zhu,^{a,b} Yaoyi Huang,^a Xiaolin Wang,^{a,b} Huichuan Yu,^{a,b} Meijin Huang,^a and Yanxin Luo^{a,b,*}

^aDepartment of Colorectal Surgery, Department of General Surgery, Guangdong Provincial Key Laboratory of Colorectal and Pelvic Floor Diseases, The Sixth Affiliated Hospital, Sun Yat-sen University, Guangzhou, Guangdong, China

^bGuangdong Institute of Gastroenterology, Guangzhou, Guangdong, 510655, China



Summary

Background More than ten randomized clinical trials are being tested to evaluate the efficacy, effectiveness and safety of a fasting-mimicking diet (FMD) combined with different antitumor agents.

Methods UMI-mRNA sequencing, Cell-cycle analysis, Label retention, metabolomics, Multilabeling et al. were used to explore mechanisms. A tandem mRFP-GFP-tagged LC3B, Annexin-V-FITC Apoptosis, TUNEL, H&E, Ki-67 and animal model was used to search for synergistic drugs.

Findings Here we showed that fasting or FMD retards tumor growth more effectively but does not increase 5-fluorouracil/oxaliplatin (5-FU/OXA) sensitivity to apoptosis *in vitro* and *in vivo*. Mechanistically, we demonstrated that CRC cells would switch from an active proliferative to a slow-cycling state during fasting. Furthermore, metabolomics shows cell proliferation was decreased to survive nutrient stress *in vivo*, as evidenced by a low level of adenosine and deoxyadenosine monophosphate. CRC cells would decrease proliferation to achieve increased survival and relapse after chemotherapy. In addition, these fasting-induced quiescent cells were more prone to develop drug-tolerant persister (DTP) tumor cells postulated to be responsible for cancer relapse and metastasis. Then, UMI-mRNA sequencing uncovered the ferroptosis pathway as the pathway most influenced by fasting. Combining fasting with ferroptosis inducer treatment leads to tumor inhibition and eradication of quiescent cells by boosting autophagy.

Interpretation Our results suggest that ferroptosis could improve the antitumor activity of FMD + chemotherapy and highlight a potential therapeutic opportunity to avoid DTP cells-driven tumor relapse and therapy failure.

Funding A full list of funding bodies can be found in the Acknowledgements section.

Copyright © 2023 The Author(s). Published by Elsevier B.V. This is an open access article under the CC BY-NC-ND license (<http://creativecommons.org/licenses/by-nc-nd/4.0/>).

Keywords: Colorectal cancer; Fasting; Quiescent cells; Ferroptosis; Drug-tolerant persister cells; Autophagy; Metabolomics

Introduction

A core hallmark of cancer cells is the dependency on specific metabolites (also called altered metabolism), and they are especially vulnerable to nutrient deprivation.¹ Fasting-mimicking diet (FMD), a plant-based, calorie-restricted, low-carbohydrate, low-protein diet to mimic a fasting-like state, has been proposed as a more feasible and safer diet. It has been proved that fasting or FMD elicits wide alterations in the tumor

microenvironment, including growth factors and metabolite levels, which might affect cancer cell metabolism to tumor growth.¹⁻³ Recently, Caffa et al. showed that FMD as an adjuvant to estrogen therapy could induce breast cancer regression.⁴ Accumulating evidence suggests that short-term fasting or FMD can render different types of cancers more vulnerable to anticancer drugs but protect healthy cells against toxic insults.^{1,5,6} In addition, numerous studies have shown

*Corresponding author. Department of Colorectal Surgery, Department of General Surgery, Guangdong Provincial Key Laboratory of Colorectal and Pelvic Floor Diseases, The Sixth Affiliated Hospital, Sun Yat-sen University, Guangzhou, Guangdong, China.

**Corresponding author. Department of Colorectal Surgery, Department of General Surgery, Guangdong Provincial Key Laboratory of Colorectal and Pelvic Floor Diseases, The Sixth Affiliated Hospital, Sun Yat-sen University, Guangzhou, Guangdong, China.

E-mail addresses: luoyx25@mail.sysu.edu.cn (Y. Luo), liuwx37@mail.sysu.edu.cn (X. Liu).

†These authors contributed equally to this work.

eBioMedicine

2023;90: 104496

Published Online xxx

<https://doi.org/10.1016/j.ebiom.2023.104496>

1016/j.ebiom.2023.104496

Research in context**Evidence before this study**

Emerging evidence supports the view that developing dietary interventions as therapy for cancer. Fasting-mimicking diet (FMD) has emerged as an attractive strategy for cancer therapies. More than ten randomized clinical trials are being tested to evaluate the efficacy, effectiveness and safety of the FMD in combination with different antitumor agents. However, whether any other antitumor agent synergizes with FMD to inhibit CRC progression and recurrence is still unknown.

Added value of this study

Here, we revealed several important new findings. ① While fasting and 5-FU/OXA can suppress the growth of CRC

tumors more effectively, the combination did not eliminate the slow-cycling cells. ② Fasting-induced quiescent CRC cells are more prone to develop drug-tolerant persister tumor cells postulated responsible for cancer relapse and metastasis. ③ Our results indicated that the FMD + ferroptosis inducer is safe and tolerable, demonstrating antitumor activity in CRC and eliminating dormant drug-resistant cancer cells.

Implications of all the available evidence

Based on our results, the FMD + chemotherapy combined with ferroptosis inducer may be an innovative therapeutic strategy for CRC patients to overcome tumor relapse by targeting proliferative tumor bulk and relatively quiescent state cells.

that dietary interventions can enhance anticancer immunosurveillance.^{2,7-9} Currently, at least ten clinical trials are evaluating the safety and efficacy of FMD combined with different anticancer drugs, including colorectal cancer, non-small cell lung cancer, breast cancer, and melanoma et al., indicating that FMD has potential application value in the prevention and treatment of cancers (<http://clinicaltrials.gov/>).

Colorectal cancer (CRC) poses a serious threat to public health, with a risk of high morbidity and mortality rates.¹⁰ Although the diagnosis and treatment of CRC were improved, such as early detection by colonoscopy, neoadjuvant therapy and immunotherapy, the 5-year survival rate remains low because of tumor metastasis or recurrence.^{11,12} Identifying and developing new therapeutic targets is imperative to overcome CRC tumor metastasis and relapse.

As the most common cancer arises from the intestine, CRC tumors undergo metabolic reprogramming, making tumor cells very sensitive to changes in the nutritional metabolism of the surrounding environment.¹³ Emerging evidence supports the view that developing dietary interventions as therapy for CRC cancer. However, is there any other antitumor agent that synergizes with FMD to inhibit CRC progression and recurrence still unknown?

Here we used UMI-mRNA sequencing, Cell-cycle analysis, Label retention experiments et al. to identify that CRC cells enter a state similar to the diapause state to evade chemotherapy-induced death under fasting conditions. Subsequently, using untargeted metabolomics, we show that FMD reduced the levels of the nucleosides/nucleotides and analogs in subcutaneous xenograft tumors, including adenosine, deoxyadenosine monophosphate and S-adenosylmethionine, indicating decreased proliferation *in vivo*. Then the transcriptional profiling reveals that the ferroptosis pathway was dysregulated in the diapause state CRC cells. We, therefore, investigate the capacity of ferroptosis inducers to improve the anti-tumor activity of

FMD + chemotherapy and highlight a potential therapeutic opportunity to avoid drug-tolerant persister cells-driven tumor relapse and therapy failure.

Methods

Cell lines and culture conditions, Reagents and antibodies, Cultivation of Primary Human CRC cells, Cell viability and Apoptosis assay, Lipid ROS detection, Organoid culture, Immunofluorescence by flow cytometry, Immunohistochemistry, Multilabeling and confocal microscopy, Quantitative RT-PCR, Iron Staining, Database analysis and UMI-mRNA sequencing and data analysis were provided in Supplementary Materials and Methods.

Animal models and drug treatments

Female Balb/c nude mice aged 4–6 weeks (~20 g) were obtained from Guangdong GemPharmatech Co., Ltd (Guangdong, China). Mice were adapted to a 12 h light/dark cycle and had free access to water. Indicated cells: HCT116 cells (3.5*10⁶), RKO cells (3.0*10⁶) and DLD1 cells (3.0*10⁶) were implanted subcutaneously into the right flank of immunodeficient nude mice. For the syngeneic model, 6-week-old female BALB/c mice (GemPharmatech Co., Ltd, China) were subcutaneously injected with 4 × 10⁵ CT26 cells resuspended in 100 μL of PBS. 7 days after inoculation, mice were randomly divided into the different experimental groups. Body weights were recorded daily, and tumor volumes were measured every 3–4 days by a digital vernier caliper according to the following equation: tumor volume (mm³) = (length × width²) × 0.5.

2 × 10⁵ MC38-Luc + cells were injected intraperitoneally into 6-week-old C57BL/6 J female mice in 100 μL of PBS. Animals were bioimaged (Xenogen IVIS system) by detecting the luciferase emission spectrum 1 week after i.p. injection to confirm the tumor growth in the peritoneum. Then, mice were randomly divided into different experimental groups. All animals were

monitored for abnormal behaviors to minimize animal suffering and pain, and the minimum number of animals necessary for the appropriate sample size was used.

Animal diets

Mice were fed ad libitum with an irradiated VRFI (P) diet (XIETONG SHENGWU, Cat#1010088) containing about 14.77 kJ/g of gross energy. The FMD diet (ReadyDietech, China) consists of two different components designated as the day 1 diet and days 2–4 diet. Day 1 diet contains 7.67 kJ/g (Cat#: RJ20082701) (provided 50% of normal daily intake; 0.46 kJ/g protein, 2.2 kJ/g carbohydrate, 5.00 kJ/g fat); the day 2–4 diet contains 1.48 kJ/g (Cat#: RJ20082702) (provided at 10% of normal daily intake; 0.01 kJ/g protein/fat, 1.47 kJ/g carbohydrates). Mice were transferred in fresh cages to avoid residual chow feeding and coprophagy before the FMD diet was supplied. Mouse weight loss did not exceed 20% by monitoring daily during the FMD cycle. Mice were fed a ketogenic diet (XIETONG SHENGWU, Cat#XTKD01) after about 18 h fasting.

Metabolomics analysis

Tumors were prepared, and metabolites were extracted. Briefly, 25 mg of the sample was homogenized with 500 μ L extract solution (acetonitrile: methanol: water = 2: 2: 1, with the isotopically-labeled internal standard mixture). After a 30s vortex, the samples were homogenized at 35 Hz for 4 min, sonicated for 5 min in an ice-water bath, and repeated thrice. Then the samples were incubated for 1 h at -40°C and centrifuged at 12,000 rpm for 15 min at 4°C . The resulting supernatant was transferred to a fresh glass vial for analysis (Biotree Biomedical Technology Co., Ltd., Shanghai, China). The quality control (QC) sample was prepared by mixing an equal aliquot of the supernatants from all samples. The metabolomics analysis was performed with LC-MS/MS, as described in previous publications.¹⁴

Fluorescent dye label retention assay

RKO or HCT116 cells were labeled with DiI (DiI18(3), Cell membrane red fluorescent probe) (Beyotime, Cat# C1036, China) according to the manufacturer's instructions. Labeled samples were treated with either a control or fasting medium for 5 days and were analyzed by flow cytometry. Negative control samples were cells that were not labeled with DiI and were used to set the gate to detect DiI. Cells not found in this gate were determined to be positive for the DiI dye label. The percentage of cells found in each gate at the indicated time points using CytExpert software.

Ethics statement

Ethical approval was gained from the Institutional Review Board of the Sixth Affiliated Hospital of Sun

Yat-sen University, China (2020ZSLYEC-231). All patients provided their written informed consent. All animal experiments complied with the ARRIVE guidelines and were operated according to protocols approved by the Institutional Laboratory Animal Care and Use Committee of The Sixth Affiliated Hospital, Sun Yat-sen University, China (IACUC-2022032401).

Statistical analysis

Data were analyzed by Student's t-test or one-way ANOVA using GraphPad Prism analytical software. The results are expressed as the mean \pm SD, and a P value < 0.05 was considered to indicate statistical significance.

Role of the funding source

The funding sources were not involved in the study design, analysis, interpretation, tissue collection, and submission decision.

Results

Combing FMD with 5-fu/oxaliplatin retards tumor growth but does not alter apoptosis sensitivity

Compared to the ad libitum (AL) diet, two FMD cycles obviously delayed tumor progression and slowed tumor growth in CT26 subcutaneous tumor model (Fig. 1a), consistent with data previously reported.^{15,16} C57BL/6 J mice bearing peritoneal murine colon cancer (MC38-luc+) were exposed to a control diet or an FMD. Although this difference was not statistically significant, there was a trend toward significance (Fig. 1b). Then, the *in vitro* fasting conditions were used to confirm our data, and fasting can significantly reduce the proliferative advantage of CRC cells (Fig. 1c). Moreover, nutrient-restricted conditions decreased organoid generation and volume (Fig. 1d). These results indicated that fasting might be a promising adjuvant treatment for colorectal cancer.

Adjuvant 5-FU-based chemotherapy combined with oxaliplatin for stage III and high-risk stage II colorectal cancer patients has demonstrated efficacy and is commonly used.¹⁷ Even though the FMD cycles can enhance gemcitabine, anti-estrogen, cyclin-dependent kinase 4 (CDK4) and CDK6 (hereafter CDK4/6) therapeutic efficacy,^{4,18} it remains unclear whether FMD combined with 5-FU/OXA has a safe and encouraging clinical activity. To explore the inhibitory effect of fasting on CRC cells when combined with 5-FU/OXA, we examined cell apoptosis using a Cell Counting Kit-8 (CCK8) and Annexin V-FITC/PI Apoptosis assays. Notably, fasting cultures treated with 5-FU/OXA showed significant growth suppression in CRC cells (Fig. 1e). However, no increase in the percentage of apoptosis was observed (Fig. 1f). The survival rates also showed no decrease with increasing 5-FU/OXA doses (10 μM , 15 μM and 20 μM) under fasting conditions

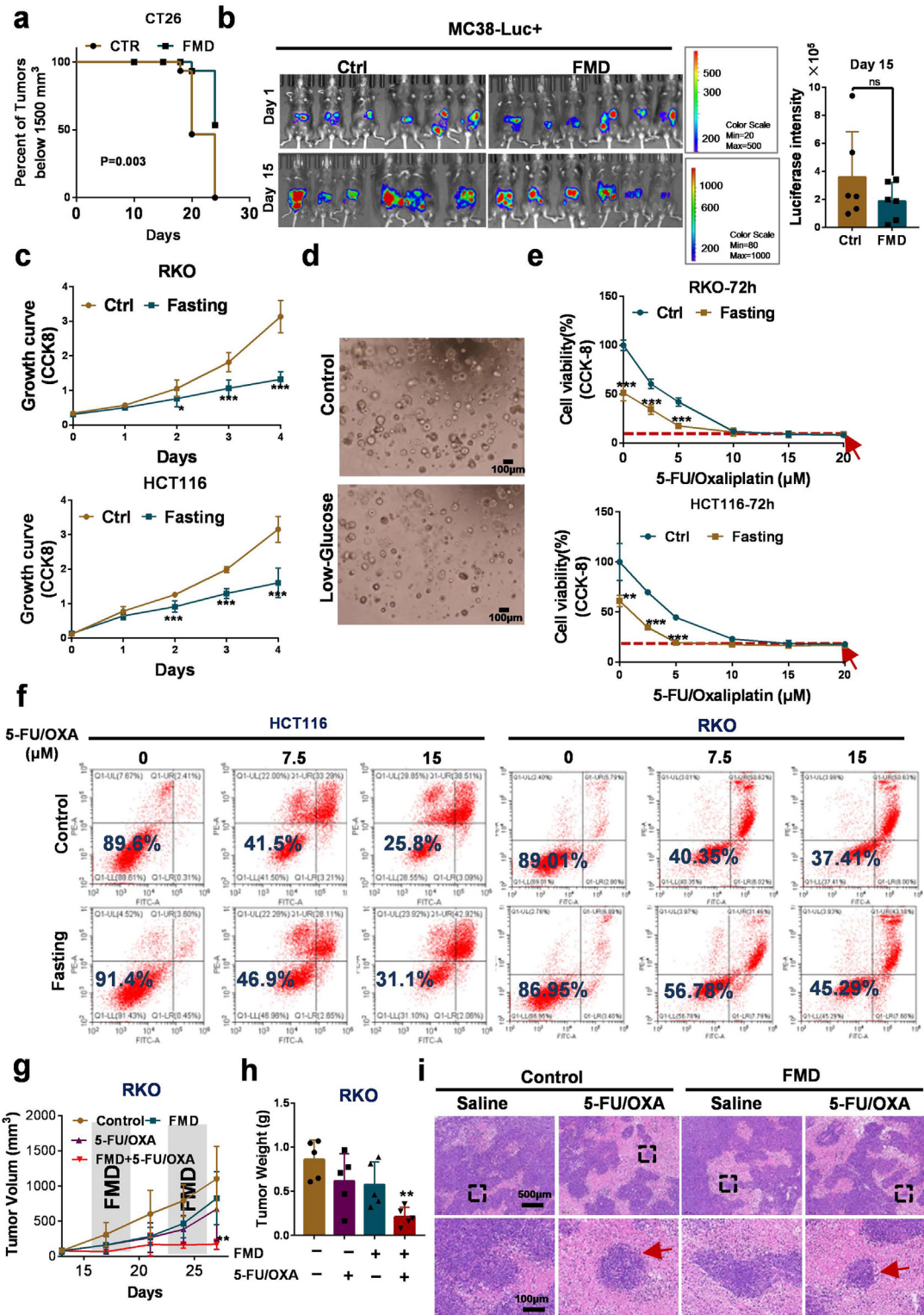


Fig. 1: Fasting impairs CRC tumor growth *in vitro* and *in vivo*, yet did not increase sensitivity to 5-FU-based chemotherapy. (a) Kaplan-Meier survival curves of Normal diet-treated (n = 7) and FMD-treated (n = 8) BalB/c mice. CT26 cells were inoculated subcutaneously into BALB/c mice. Mice were sacrificed when the tumor volume reached 1500 mm³. P-value was derived from the log-rank test. (b) The antitumor effect of

(Fig. 1e, red arrow). Similarly, fasting did not enhance the inhibitory effect of 5-FU alone on tumor growth, even at a high concentration (50–200 μM) (Fig. S1a–b). To further verify the effect of FMD on 5-FU-based chemotherapy observed *in vitro*, we subcutaneously injected RKO cells into BALB/c nude mice. The FMD synergized with 5-FU/OXA appreciably attenuated tumor growth in the mice. The final tumor weights and volumes in the FMD+5-FU/OXA group were markedly lower than those in the other groups (Fig. 1g–h, Fig. S1c–d). However, despite FMD + 5-FU/OXA treated tumors ceased to grow, the necrotic/apoptotic areas were not expanded compared with 5-FU/OXA by the Hematoxylin/eosin (H&E) staining (Fig. 1i), as evident by shrinkage and nuclear condensation indicative of apoptosis. This result was consistent with our *in vitro* finding that fasting retarded tumor growth but did not increase 5-FU/OXA sensitivity to apoptosis in CRC. In addition, clusters of viable tumor cells in the necrotic/apoptotic regions can be found (Fig. 1i, red arrow), likely to be a source for tumor recurrence and resistance.

Nutrient-restricted conditions drive CRC cells to enter a quiescent state to resist chemotherapy

Fasting/FMD can protect normal cells and organs but sensitize different cancer cell types to chemotherapy.¹ However, here we showed that fasting did not potentiate the anti-tumor effect of 5-FU/OXA, which appears to be in conflict with the previous finding. This observation prompted us to investigate the possible cause(s). We next performed an UMI-mRNA sequencing experiment on RKO cells to evaluate the effect of low glucose and low FBS treatment. As shown in Fig. 2a and b, pathway enrichment analysis identified that upregulated genes significantly enriched in Protein processing in endoplasmic reticulum, Ribosome, and RNA transport; but a significant decrease in cell proliferation pathways, including DNA replication and Cell cycle et al. Gene ontology analysis of these downregulated genes, revealed that cell cycle and cell division et al. were among the most significantly enriched pathways (Fig. 2c). Key genes involved in proliferation (MKI67, CDK1) and DNA replication (PCNA) were all downregulated (Fig. 2d). However, among the most upregulated genes in fasting-treated CRC cells, we identified

genes linked to stemness: RUNX1, KLF4, CD44, ALDH2 and ALDH6A1^{19,20}; and related to chemoresistance: RBCK1, RAE1, NR4A2 and KDM5B^{20–24} (Fig. 2d). Label retention experiments were used to confirm whether these cells entered a low proliferative state under fasting conditions. The result revealed that dilution of the DiI dye at a much slower rate in fasting-treated cultures compared with control cultures (Fig. 2e, Fig. S2a). Similarly, we found that fasting caused a decrease in the fraction of cells in the S phase (Fig. 2f, Fig. S2b). Additionally, fasting-treated cells showed a significant decrease in total RNA abundance (Fig. 2g, Fig. S2c), indicating the global suppression of transcription.^{25,26} These data suggested that the fasting-induced dormant state may be important in endowing chemoresistance to CRC cells.

It has been reported that FMD affects various metabolic and endocrine parameters *in vivo*.²⁷ Subsequently, we measured metabolite abundance in two subcutaneous tumor models: CT26 and HCT116, using LC-MS/MS-based metabolomics. Interestingly, OPLS-DA analysis revealed a clear difference in metabolic profiles between the tumor tissues collected from FMD-fed and normally-fed mice regardless of which cell line was used (Fig. 3a, Fig. S3a). As shown in Fig. 3b and Supplementary Fig. 3b, the permutation test of the OPLS-DA model showed no overcorrection phenomenon, suggesting that the model was suitable and the differential metabolites were reliable. Among these metabolites, the levels of Lipids and lipid-like molecules, Organic acids and derivatives, Organic compounds et al. were increased. However, FMD reduced adenosine and deoxyadenosine monophosphate levels, indicating decreased proliferation (Fig. 3c, Fig. S3c) as the nucleosides/nucleotides and analogs are the most abundant metabolic substrates for providing essential components to synthesize DNA/RNA and the necessary energy and cofactors to promote cell proliferation (Tables S1 and S2). These suggested that FMD can induce a metabolic switch from using glucose as a fuel source to using fatty acids and lipids et al., and decreased cell proliferation to survive nutrient stress.

In addition, tumors from mice treated with 5-FU/OXA and FMD+5-FU/OXA appeared to have more necrotic or apoptotic regions by H&E staining (Fig. 1i)

FMD was determined in the MC38-Luc + peritoneal model. Animals were bioimaging (Xenogen IVIS system) by detecting the luciferase emission spectrum at 2 weeks. $n = 6$. P-values were calculated by two-tailed paired t-test. (c) The proliferation of HCT116 cells (upper panel) and RKO cells (lower panel) under fasting conditions was measured by a CCK8 assay. $n = 3$. P values were calculated by two-tailed paired t-test. (d) Representative pictures of colon organoids under nutrient-restricted conditions for 48 h were shown. $n = 3$. (e) Cell survival was measured by a CCK8 assay after the indicated treatment for 72 h. $n = 3$. P values were calculated by two-tailed paired t-test. (f) Apoptosis was assessed by annexin-V/PI assay by FACS analysis after the indicated treatment for 72 h. The value in each panel indicates the % of surviving cells. Data are representative of three independent experiments. (g) Tumor growth and (h) weight of RKO cells inoculated subcutaneously in Balb/C nude mice treated with 5-FU/OXA (25 mg/kg 5-FU and 2.5 mg/kg OXA; i.p.; twice/week), FMD, their combination or vehicle (control) was shown. $n = 5$ per group. P values were calculated by one-way ANOVA. (i) Tumor tissues were fixed, sliced, and stained with H&E for pathological analysis. Scale bar: 500 μm (upper panel); 100 μm (lower panel). Bars, mean \pm SD. * $p < 0.05$, ** $p < 0.01$, *** $p < 0.001$.

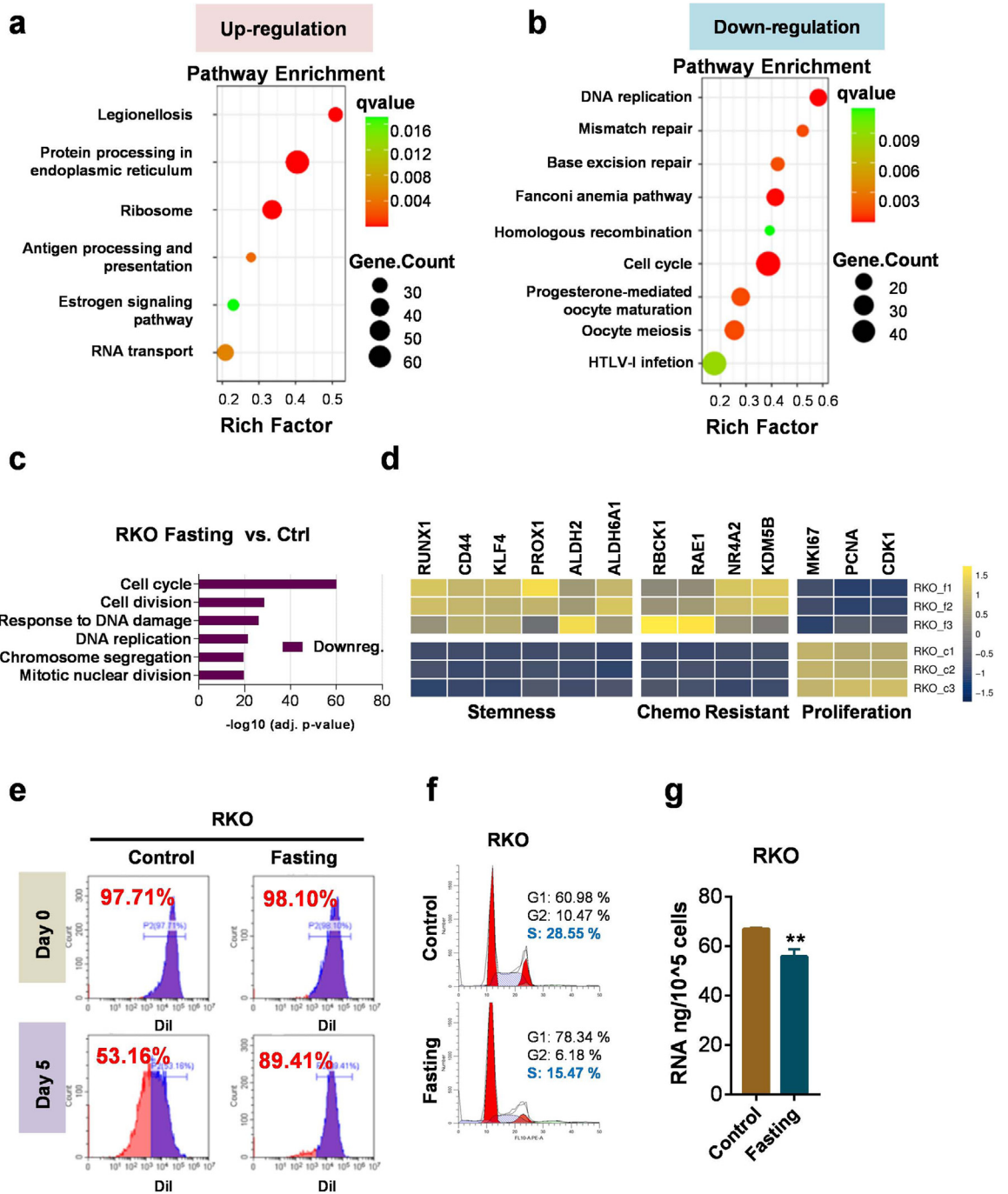


Fig. 2: CRC cells treated with fasting that escape from the chemotherapeutic agent killing are quiescent. (a–b) The KEGG pathway analyses the enriched terms of significantly upregulated (a) or downregulated (b) genes in RKO cells after the control or fasting treatment for 48 h. n = 3. (c) Pathway enrichment analysis from (b) focused on cell proliferation-related pathways. (d) UMI-mRNA sequencing analysis of RKO cells with the indicated treatment. Heatmaps show differentially expressed genes involved in stemness, chemotherapy resistance and Proliferation. (e) RKO cells with the indicated treatment incubated with Cell Plasma Membrane Staining DiI18(3) for 0 and 5 days were analyzed by flow cytometry. Data are representative of three independent experiments. (f) Cell cycle analysis of RKO cells treated with control or fasting medium for 72 h was detected by flow cytometry. Data are representative of three independent experiments. (g) RNA abundance was measured by NanoDrop Microvolume Spectrophotometers after control or fasting 48 h treatment. n = 3. Bars, mean ± SD. **p < 0.01, P values were calculated by two-tailed paired t-test.

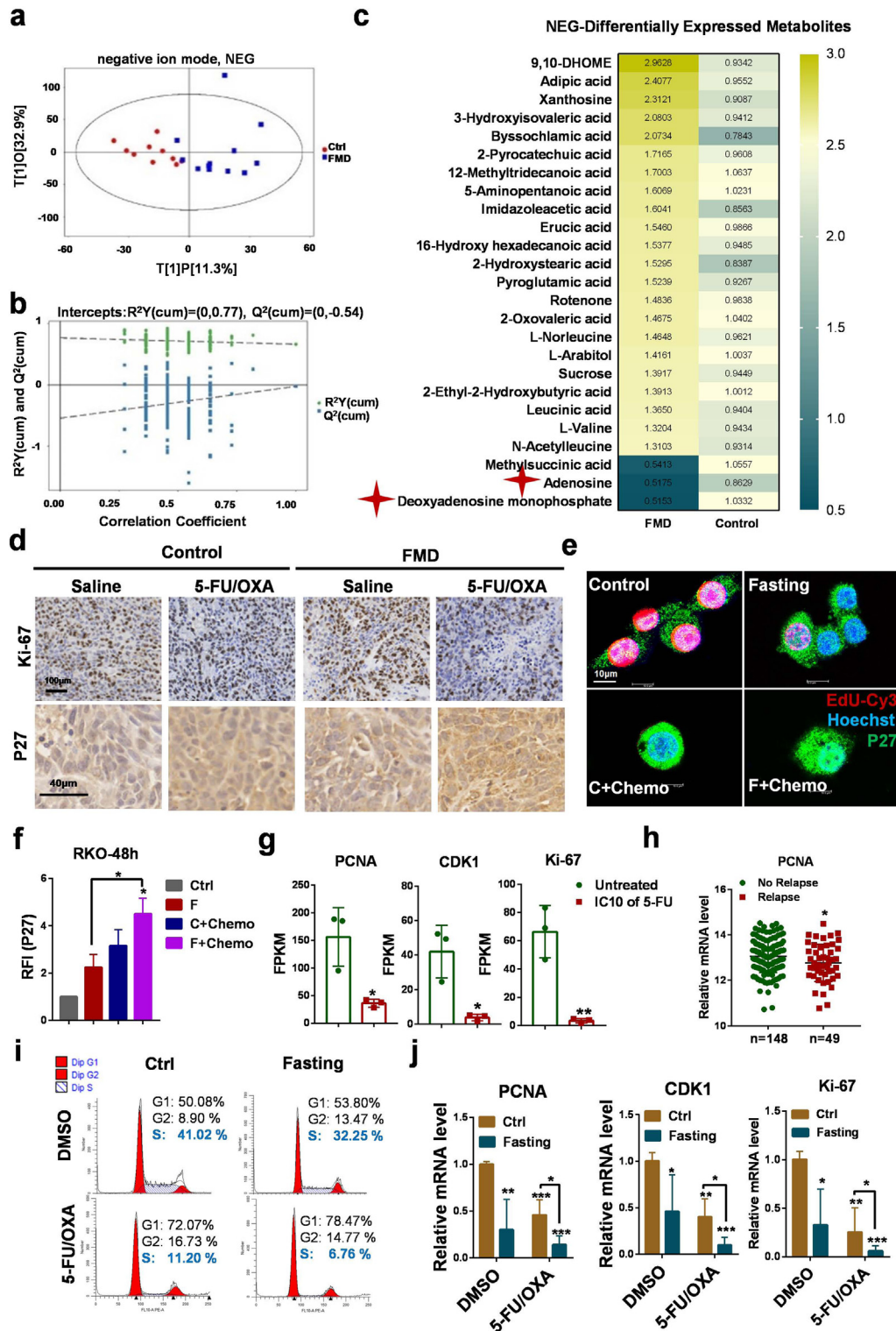


Fig. 3: The residual tumor cells that exit proliferation and enter quiescence to survive under pressure from chemotherapy. (a) Score scatter plot of OPLS-DA model for group CTR (n = 10) vs. FMD (n = 12) by negative ion mode. (b) Permutation test of OPLS-DA model for group CTR (n = 10) vs. FMD (n = 12) by negative ion mode. (c) Heatmaps showed differentially expressed metabolites in tumors measured by

accompanied by decreased proliferation by Ki-67 staining compared to corresponding controls, especially in FMD+5-FU/OXA group (Fig. 3d, upper panel). It is well-known that degradation of P27 (also named CDKN1B or KIP1), a cyclin-dependent kinase inhibitor, is required for the cellular transition from quiescence to the proliferative state. Indeed, surviving cells in the necrotic or apoptotic regions formed clusters from 5-FU/OXA and FMD+5-FU/OXA treated groups expressing higher P27 (Fig. 3d, lower panel). Next, immunofluorescence and flow cytometry was performed to show that surviving cells in the presence of chemotherapeutics were at a higher level of P27 (Fig. 3e–f, Fig. S3d–e). However, the EdU signal was negative (Fig. 3e, Fig. S3d), suggesting that a quiescent state may increase constitutive survival signals in CRC cells. We analyzed GEO datasets (GSE193865) and showed that the tumor cells could survive long-term exposure to low-dose 5-FU are slow-cycling (Fig. 3g). Importantly, analysis of the public database (GSE87211) revealed that CRC patients who received 5-FU-based chemotherapy after surgery with recurrence had lower expression of PCNA (DNA replication marker) (Fig. 3h). Then, our data also revealed that CRC cell survival or drug tolerance after 5-FU/OXA treatment had a decrease in the percentage of cells entering S-phase of the cell cycle and the expression of genes associated with cell proliferation, especially the group of fasting+5-FU/OXA (Fig. 3i–j, Fig. S3f–g). These results demonstrated that tumor cells with a quiescent state likely contributed to their resistance to chemotherapy, which was consistent with observations reported previously.^{26,28}

Fasting-induced quiescent CRC cells are more prone to develop drug-tolerant persister tumor cells

Drug-tolerant persister (DTP) cells, a subpopulation of cells adapted to survive in response to chemotherapy or targeted agent with nonmutational mechanisms that drive drug tolerance, present a major hurdle to successful cancer therapy.^{26,29} One of the important characteristics of DTP cells is quiescent or slow-cycling to survive cytotoxic agent exposure. Primary CRC cells derived from patient-derived tissue resections were used to determine whether fasting-induced quiescent state

plays a role in driving the DTP state. Immunofluorescence results showed that α -SMA expression was negative, whereas cytokeratin expression was positive in the targeted cells (Fig. 4a), suggesting pure primary CRC cells were obtained. CCK8 assay showed that no statistical differences were observed under the high dose of 5-FU/OXA (10, 15 and 20 μ M) among the control and fasting group (Fig. 4b). In addition, despite a slight increase in the cytotoxic effect of 5-FU/OXA in primary CRC cells under fasting conditions using flow cytometry analysis of apoptotic cell death and were not statistically different from each other, a large population of viable cells remained (Fig. 4c, Fig. S4a–b). Then, the DTP cells model was introduced, as described in Fig. 4d, to evaluate the influence of fasting on persister cell generation. The data showed that a small population of primary CRC cells, about 10%, entered a persister state to evade the cytotoxic of 5-FU/OXA (Fig. 4d). About 30 days after removal of 5-FU/OXA allowed the persister cells to regrow. Persister cells from control cultures re-acquire sensitivity to 5-FU/OXA, whereas fasting cultures derived-drug-tolerant cells showed more resistance to 5-FU/OXA (Fig. 4e and f). This result implied that a dormant state is believed to contribute to developing resistance or persister cells if tumor cells cannot be killed under starvation conditions.

CRC cells that enter a quiescent state to resist chemotherapy are vulnerable to ferroptosis

Ferroptosis was originally defined as an iron-dependent form of cancer cell death.³⁰ Based on UMI-mRNA sequencing results, we showed that eleven of the top 25 most changed genes (P-value) after fasting treatment were implicated in regulating ferroptosis, endoplasmic reticulum (ER) stress or belonging to heat shock protein (HSP) family (Fig. 5a). Interestingly, ER stress and HSPs play an important role in the occurrence and development of ferroptosis.^{31–33} Moreover, according to the fold change, four of the top 20 most significantly up-regulated genes were reported to be involved in ferroptosis (Fig. 5b and c), including ferroptosis-promoting (HMOX1, PTGS2) and ferroptosis-inhibiting (NUPR1, SLC7A11). It is reasonable to expect that nutrient-deprivation-induced quiescent cells may be sensitive to

negative ion mode. P values were calculated by two-tailed paired t-test. (d) Representative images of Ki-67 staining (upper panel) and Immunohistochemistry analysis of the residual tumor cells (subcutaneous RKO tumors, Fig. 1i) in the indicated tumors-expressing P27 level (lower panel). n = 5. (e) EdU labeling and P27 staining in the residual viable RKO cells after 5FU/OXA treatment for 48 h. Data are representative of two independent experiments. Scale bar: 10 μ m. (f) Flow cytometry analysis of P27 expression in RKO cells with indicated treatment for 48 h. n = 3. P values were calculated by one-way ANOVA. RFI: relative fluorescence intensity. (g) Bar plots show differentially expressed genes involved in the proliferation of survival HCT8 cells after treatment with low dose 5FU from the GSE193865 database. n = 3. P values were calculated by two-tailed paired t-test. (h) Scatter plot of PCNA expression in CRC patients who received neoadjuvant chemotherapy with recurrence (n = 49) and no recurrence (n = 49) based on the GSE87211 database. P values were calculated by two-tailed paired t-test. (i) Cell cycle analysis of RKO cells with indicated treatment for 48 h was detected by flow cytometry. Data are representative of three independent experiments. (j) Relative mRNA expression of the indicated genes in RKO cells with indicated treatment for 48 h. n = 3, P values were calculated by two-tailed paired t-test. Bars, mean \pm SD. *p < 0.05, **p < 0.01, ***p < 0.001.

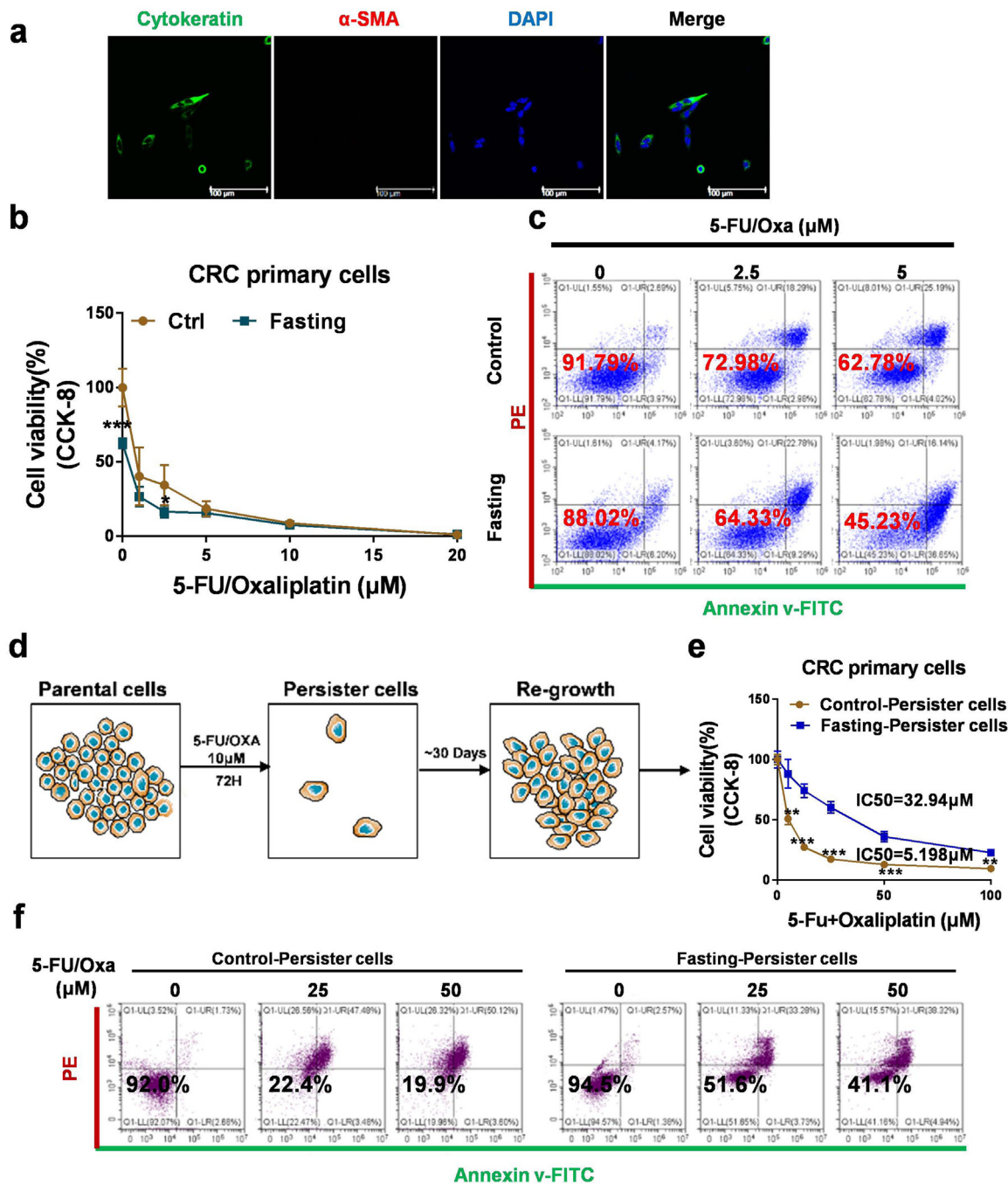


Fig. 4: Fasting-induced quiescent CRC cells are more prone to develop drug-tolerant persister tumor cells. (a) Immunofluorescence staining of Cytokeratin and α -SMA in primary CRC cells isolated from colon cancer tissues. $n = 3$. (b) CRC primary cells were treated with various concentrations of 5-FU/OXA under control or fasting conditions for 72 h and then subjected to CCK8 assay, $n = 3$. P values were calculated by two-tailed paired t-test. (c) Apoptosis was assessed by annexin-V/PI assay by FACS analysis after treatment under the indicated conditions for 72 h. The value in each panel indicates the % of surviving cells. Data are representative of three independent experiments. (d) Schematic illustration of the construction of primary CRC persister cells. Scale bars indicate 50 μ m. (e) Indicated persister cells were treated with various concentrations of 5-FU/OXA for 72 h and then subjected to CCK8 assay, $n = 3$. P values were calculated by two-tailed paired t-test. (f) Indicated persister cells were treated with various concentrations of 5-FU/OXA for 72 h and then subjected to apoptosis assay by annexin-V/PI. The value in each panel indicates the % of surviving cells. Data are representative of two independent experiments. Bars, mean \pm SD. *** $p < 0.001$.

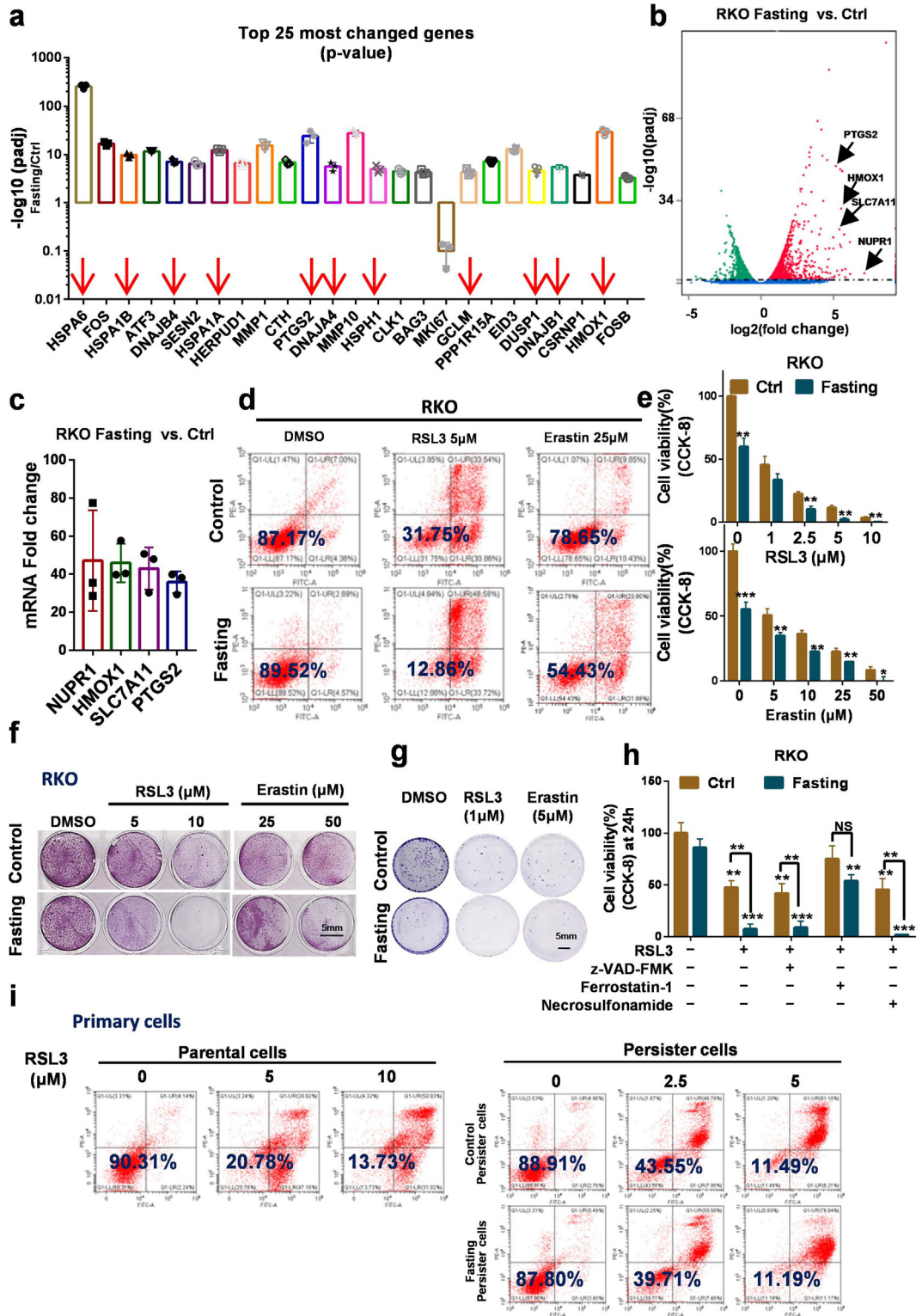


Fig. 5: UMI-mRNA sequencing implicates fasting and ferroptosis synergize to promote tumor death. (a) The top 25 (identified by lowest P-value) significantly differentially expressed genes were shown from the analysis of UMI-mRNA sequencing. n = 3. (b) Volcano plot of significant differentially expressed genes. (c) Four of the top 20 significantly changed genes involved in the ferroptosis pathway were analyzed by UMI-

ferroptosis inducers. Indeed, we observed that fasting cultures enhanced the antitumor effect of Erastin and RSL3 against all tested CRC cell lines *in vitro* by Apoptosis Assay, Crystal Violet Staining, CCK8 and Colony formation (Fig. 5d–g, Fig. S5a–d). Consistently, cell death induced by RSL3 only could be rescued by ferrostatin-1 (ferroptosis inhibitor), but not z-VAD-FMK (apoptosis inhibitor), necrostatin-1 (necroptosis inhibitor) (Fig. 5h, Fig. S5e). Then, we wondered whether persister cells with a preferential vulnerability to ferroptosis. Our data showed that persister cells were more sensitive to the ferroptosis inducer-induced cell death (Fig. 5i, Fig. S5f–g). Following the increased ferroptotic cell death in CRC cells, it was further detected that the intracellular iron levels were obviously higher (Fig. 6a, Fig. S6a), suggesting specific effects of fasting on regulating the ferroptosis response in CRC cells. Furthermore, we showed that fasting cultures promoted ferroptosis by increasing lipid ROS production (Fig. 6b, Fig. S6b). Previous reports have shown that nutrient deprivation activates autophagy.^{34,35} Importantly, autophagy contributes to ferroptotic cell death.^{36,37} We hypothesized that autophagy played an important role in fasting and sensitized cells to ferroptotic cell death. As expected, Erastin and RSL3 treatment significantly induced the expression of a universal autophagy marker (LC3B) under fasting conditions (Fig. 6c, Fig. S6c). Subsequently, a tandem mRFP-GFP-tagged LC3B construct was used to confirm this observation. Notably, we observed that fasting + RSL3 or Erastin markedly increased the number of LC3B puncta (GFP + RFP+) in CRC cells, a large proportion of yellow puncta, reflective of RFP+ and GFP + signal (autophagosomes) (Fig. 6d–e, Fig. S6d–e), suggesting increased induction of autophagy. Indeed, when autophagy in normal cultures treated RKO cells were activated by rapamycin, their apoptotic response to RSL3 was significantly increased with only 14.89% viable cells (Fig. 6f, Fig. S6f). The RSL3-induced cell death under fasting cultures could be rescued by the ferroptosis inhibitor ferrostatin-1, Liproxstatin-1 (Fig. 6g, Fig. S6g). Additionally, blocking the early-stage autophagic flux by wortmannin could partially protect from fasting + RSL3-induced apoptosis (Fig. 6g, Fig. S6g).³⁸ Altogether, these findings demonstrated that induction of autophagy by fasting promotes

cellular lipid ROS accumulation upon ferroptosis by increasing free iron levels in cells and contributes to ferroptosis inducer-mediated CRC cell death.

Dietary interventions enhance the antitumor effects of ferroptosis *in vivo*

FMD cycles can enhance cancer therapy. Dietary interventions could improve tumor therapy by eliminating specific nutrients, modulating growth factors, and altering the systemic immune state to affect tumor growth and the antitumor immune response et al.^{13,39} Thus far, we have shown that fasting can induce autophagy and promote ferroptosis *in vitro*. Next, we investigated whether FMD cycles enhance the anticancer activity of ferroptosis inducers *in vivo*. Compared with standard diets, all FMD groups displayed some degree of inhibitory effect on growth (Fig. 7a–c). However, the inhibition was not statistically significant at the end time point, except for group FMD + RSL3+5FU (Fig. 7b and c). Of note, triple treatment (FMD + RSL3+5-FU) was the most active therapeutic intervention in delaying tumor progression in a mouse xenograft, accompanied by increased Fe²⁺ accumulation (Fig. 7d) and augmented apoptosis via TUNEL and H&E staining (Fig. 7e and f). Fe²⁺ levels did not increase in the FMD + RSL3 group, which may result from a large amount of necrosis/apoptosis causing liquefaction and exudation of the tumor tissue during sampling. Furthermore, according to the results of H&E staining for intact tumors (Fig. 7f), necrosis/apoptosis occurred in all of the FMD group xenografts in the process of tumor treatment. Importantly, foci of residual viable tumors in the areas of tumor necrosis were barely visible in the FMD + RSL3 and FMD + RSL3+5FU treated tumors. These data indicate that FMD cycles sensitize to RSL3-induced ferroptosis and tumor suppression *in vivo*, especially plus the chemotherapeutic agent 5-FU. These results indicated that RSL3 could further potentiate the effects of chemotherapy + FMD against quiescent CRC cells that resist chemotherapy.

There is growing enthusiasm for using very low carbohydrate (ketogenic) diets (KD) as an anticancer intervention. As a potential pharmacologic partner of PI3K–mTOR pathway inhibitor, KD can activate AMP-activated protein kinase (AMPK)⁹ and enhance

mRNA sequencing. n = 3. (d) RKO cells were treated with the RSL3 or Erastin and fasting + RSL3 or fasting + Erastin for 24 h and subjected to annexin-V/PI assay. The values within each panel indicate % of survival cells. Data are representative of two independent experiments. (e) Comparison of the sensitivity of RKO cells to ferroptosis inducers under control or fasting cultures. Cell viability was measured by CCK8 assay after treatment under the indicated conditions for 24 h n = 3. (f) RKO cells were stained with crystal violet after treatment under the indicated conditions for 24 h. Data are representative of two independent experiments. Scale bars indicate 5 mm. (g) Colony formation assay. RKO cells were grown for 14 days in the presence of Erastin (5 μM) or RSL3 (1 μM) under control or fasting conditions. n = 3. Scale bars indicate 5 mm. (h) The reversal effect by the indicated inhibitors on 5 μM RSL3-induced ferroptosis. Cell viability was measured by CCK8 assay after treatment under the indicated conditions for 24 h n = 3. ferrostatin-1 (1 μM), z-VAD-FMK (10 μM), necrostatin-1 (1 μM). (i) Parental and persister cells were treated with the RSL3 for 24 h and subjected to annexin-V/PI assay. The values within each panel indicate % of survival cells. n = 3. Bars, mean ± SD. *p < 0.05, **p < 0.01, ***p < 0.001, P values were calculated by two-tailed paired t-test.

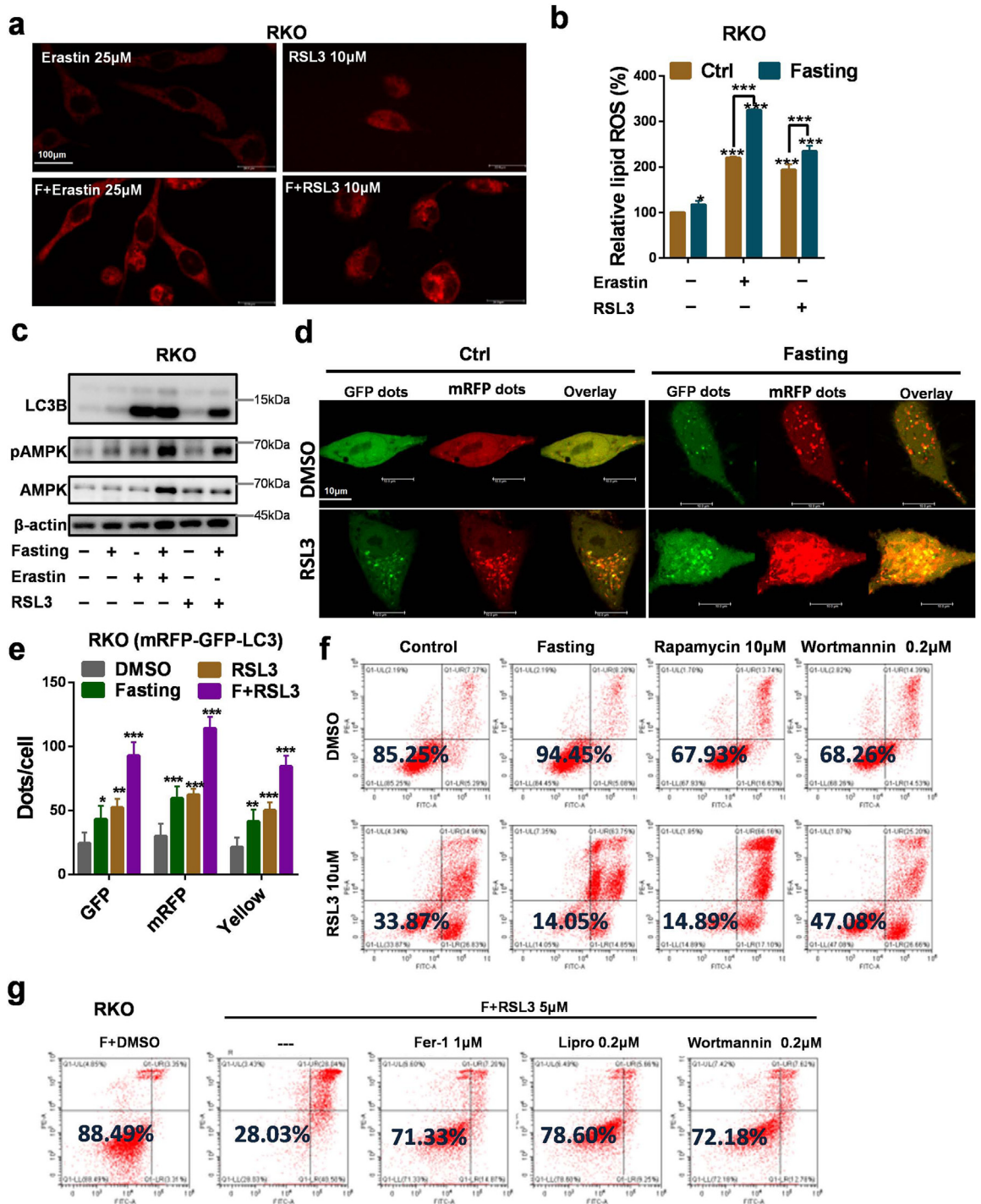


Fig. 6: Fasting-induced autophagy promotes ferroptosis. (a) Fe²⁺ levels were measured in RKO cells after treatment under the indicated conditions for 18 h by confocal laser microscopy. F: fasting. n = 3. Scale bar: 100 µm. (b) Lipid ROS levels were measured in RKO cells after treatment under the indicated conditions for 15 h by BODIPY C11 staining. n = 3. (c) Western blot detected protein expressions after the indicated treatment for 24 h. Data are representative of two independent experiments. (d) Immunofluorescence analysis of RKO cells transfected with tandem mRFP-GFP-tagged LC3B after treatment under the indicated conditions for 24 h. Scale bar: 10 µm. n = 3. mRFP-GFP-LC3 adenoviral vectors were purchased from HanBio Technology (Shanghai, China). (e) Quantifying the ratio of red puncta indicating autolysosome versus yellow puncta indicating autophagosome in (d). (f–g) Apoptosis was assessed by annexin-V/PI assay by FACS analysis after treatment under the indicated conditions for 24 h. The value in each panel indicates the % of surviving cells. Fer-1: Ferrostatin-1; Lipro: Liproxstatin-1. Data are representative of two independent experiments. Bars, mean ± SD. *p < 0.05, **p < 0.01, ***p < 0.001, P values were calculated by two-tailed paired t-test.

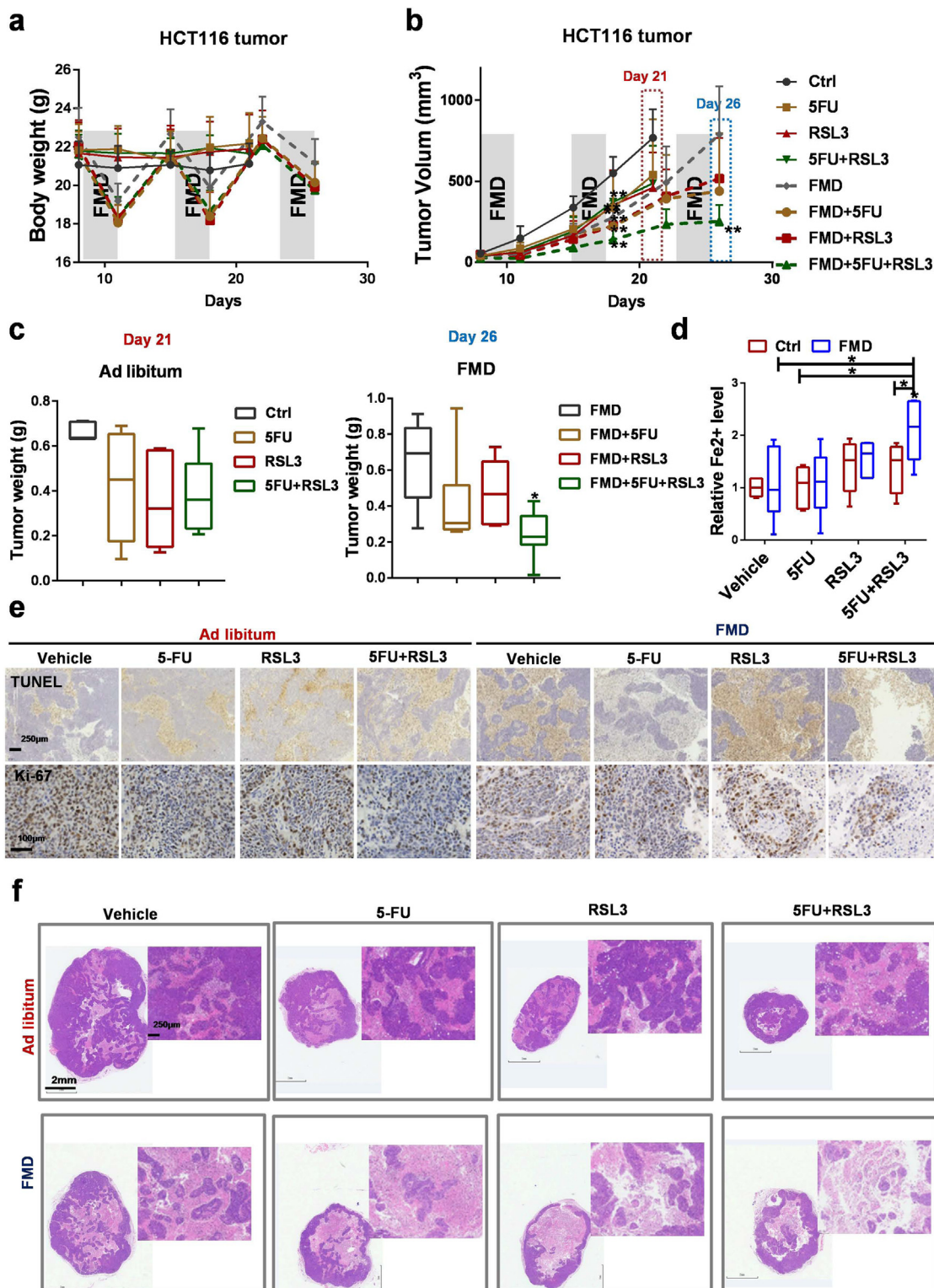


Fig. 7: Fasting-mimicking diet synergizes with RSL3/5-FU against quiescent cancer cells that resist chemotherapy. (a-c) Mice bearing HCT116 xenograft tumors were fed ad libitum or subjected to FMD cycles and treated with the indicated agents. *n* = 6 or 7 per group. RSL3:100 mg/kg, i.p.; twice per week. (a) Body weight, (b) Tumor growth, (c) Tumor weight are presented. (d) Fe²⁺ concentrations were

autophagy⁴⁰ by inducing energy deprivation. We further demonstrated that the KD combined with Erastin was more efficient than Erastin alone in inhibiting tumor growth in another CRC model that subcutaneously implants DLD1 cells (Fig. 8a–d). In addition, clusters of viable tumor cells in the necrotic/apoptotic regions obviously decreased (Fig. 8e). Collectively, our data support the idea that activation of autophagy effectively enhances the anticancer activity of ferroptosis inducers *in vivo*, especially contributing to persister cells' ferroptotic death and presenting a potential strategy to prevent tumor relapse *in vivo*.

Discussion

Multiple preclinical and randomized clinical trials have demonstrated that FMD enhances the antitumor activity of chemotherapy agents and immunotherapy in various malignancies.^{2,4,5,16,41–44} Adiposity could lie along a causal pathway from dietary pattern to colon cancer.⁴⁵ Tabung et al. showed that dietary patterns were associated with colorectal cancer development.⁴⁶ Klurfeld et al. proposed that calorie restriction can inhibit CRC tumor growth as early as 1987.⁴⁷ In our study, tumor growth inhibition was also apparent besides FMD being safe, well tolerated and feasible in combination with 5-FU/OXA. Strikingly, fasting cannot increase apoptosis triggered by 5-FU/OXA in CRC cells *in vitro*, and the findings we could confirm in a subcutaneous xenograft mouse model *in vivo*. Clusters of residual viable tumors in the apoptotic regions were visible in the FMD+5FU/OXA-treated tumors.

Since several reports have previously shown that nutrient-deficient conditions would induce and select cancer stem cells adapted to survive, promote stemness programs, drive cells to enter a quiescent state and become tolerant to drugs.^{28,48,49} Then we speculated that the capability of cancer cells to escape the cytotoxic effect of the chemotherapeutic drug in fasting cultures resulted from a dormant state since starving cells have to exit proliferation and enter quiescence. Using UMI-mRNA sequencing, cell-cycle analyses, label retention experiments, EdU staining and metabolomics, we further revealed that CRC cells are slow-cycling under a nutrient-deficient environment, consistent with previous reports.^{28,50,51}

Subsequently, metabolomics revealed that metabolites were consistently altered in the subcutaneous tumors arising from different cell types between the two groups. On the one hand, a shift of the energy source to maintain cellular energy and survival during fasting. On the other hand, tumor growth and cell proliferation slow down to

cope with nutrient deficiency. The animal experiments confirmed that CRC cells escaped being killed by 5-FU/OXA and formed clusters of quiescent cancer cells expressing a higher level of P27 but a lower level of ki-67. Long-term exposure to chemotherapeutic drugs would cause the development of resistance, and we observed that CRC cells mitigated the cell-killing effects of low-dose 5-FU by decreased proliferative capacity (GSE193865). Furthermore, we analyzed GEO datasets to confirm that slowing cell proliferation in chemotherapy patients contributes to relapse and disease progression (GSE87211). Rehman et al. demonstrated that CRC cells enter a diapause-like drug-tolerant persister state to survive chemotherapy.²⁶ We also consistently found that survival of the live CRC cells after the chemotherapy challenge had a significantly low gene expression level involved in proliferation, and S phases concomitantly decreased. In light of a recent publication, Baldominos et al. showed that quiescent cancer cells form clusters with reduced immune infiltration and resist T-cell attack.²⁰ Using patient-derived xenografts (PDXs), Echeverria et al. also revealed that only the quiescent or slow-cycling cancer cells could repopulate the tumor after neoadjuvant chemotherapy.⁵² Sarah et al. revealed that dormant human ALL cells displayed drug resistance and can survive drug treatment that exhibits typical challenging adverse characteristics of relapse induction.⁵³

The dormancy of cancer cells is becoming more widely recognized as an important clinical issue. A recurring question is whether tumor cells that become dormant in fasting cultures would be more prone to generate persister cells and confer drug resistance. Then we reinforced this hypothesis by using primary human CRC cells. A mild decline ($P > 0.5$) in the proportion of surviving cells in the fasting group that might result from primary cells in the *ex vivo* system was less adaptive to cope with stress during 5-FU/OXA treatment. However, due to the high heterogeneity in the initial primary cell population, nutrient deprivation can drive small subpopulations of primary cells into a quiescent state to survive the chemotherapeutic stress and enter a drug-tolerant 'persister' state, promoting the emergence of resistance. Notably, residual or dormant tumor cells may be the primary cause of eventual resistance and recurrence after therapy. Consequently, some studies showed that targeting dormant cancer cells is a promising approach to overcoming cell-intrinsic drug resistance and preventing disease relapse.^{54–57}

Since fasting/FMD is known to be safe and efficacious in treating tumors, efforts are needed to develop

measured in tumor tissues. (e) TUNEL staining (upper) and Ki-67 staining (lower) in tumor tissues from different treatment groups. (f) Cross-sections of tumors were H&E stained (Bottom left panel, Scale bar: 2 mm); Magnified H&E images (upper right panel, Scale bar: 250 μ m). Bars, mean \pm SD. * $p < 0.05$, P values were calculated by two-tailed paired t-test or one-way ANOVA.

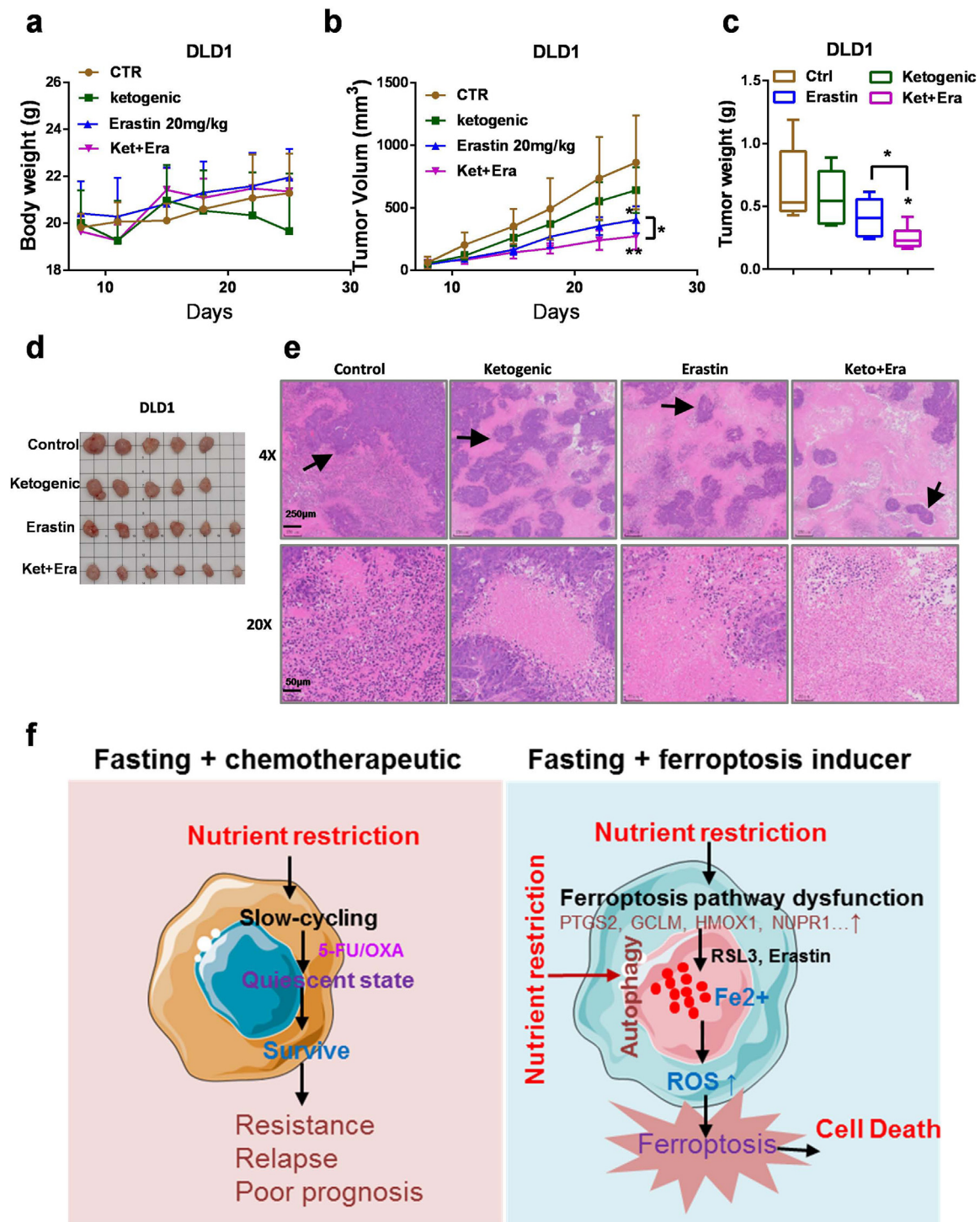


Fig. 8: A ketogenic diet sensitizes CRC cancer to ferroptosis and significantly reduces the number of residual viable tumor foci. (a–c) Mice bearing DLD1 xenograft tumors were fed a ketogenic diet and treated with or without Erastin. Erastin: 25 mg/kg, i.p.; once a day. (a) Body weight, (b) Tumor growth curve, (c) Tumor weight and (d) Tumor images are presented. $n = 5$ or 6 . (e) Representative images of H&E staining of the resected tumor. The residual viable tumor was present (marked by arrows). (f) The schematic diagram shows how nutrient restriction synergizes with ferroptosis to promote apoptosis and eliminate dormant drug-resistant cancer cells. Bars, mean \pm SD. * $p < 0.05$, ** $p < 0.01$. P values were calculated by one-way ANOVA.

more efficient approaches to block drug resistance and recurrence. Using UMI-mRNA sequencing, we discovered that the ferroptosis pathway was already dysregulated in CRC cells under fasting conditions. Combination treatment of fasting and ferroptosis inducers significantly promotes CRC cell death, including quiescent cancer cells, providing insight into therapeutic opportunities to target cancer cells in the dormant state. Notably, drug-tolerant persister cancer cells derived from human primary colorectal cancer cells and RKO cell lines are vulnerable to the ferroptosis inducer. In addition to ferroptosis being a form of autophagic cell death, autophagy promotes ferroptosis, which has been extensively documented.^{37,58–60} Our data revealed that fasting-induced autophagy benefits ferroptosis inducers by increasing Fe²⁺ accumulation and lipid ROS production, supporting autophagy's causal role in the anti-CRC effect of ferroptosis. Importantly, fasting can synergize with ferroptosis inducers to eliminate dormant drug-resistant CRC cells *in vivo*. In mice, two cycles of FMD or a ketogenic diet that stimulates autophagy induction⁶¹ can increase the antitumor activity of ferroptosis inducers and eliminate dormant cancer cells induced in the nutrient-deficient tumor microenvironment.

Our study revealed several important new findings. ① While fasting and 5-FU/OXA can suppress the growth of CRC tumors more effectively, the combination did not eliminate the slow-cycling/quiescent cells. ② Fasting-induced quiescent CRC cells in energy stress conditions are more prone to develop drug-tolerant persister tumor cells. ③ Our results indicated that the FMD/ketogenic diets + ferroptosis inducer is safe and tolerable, demonstrating antitumor activity in CRC and eliminating dormant drug-resistant cancer cells.

Collectively, FMD + chemotherapy combined with ferroptosis inducer may yield better outcomes to effectively inhibit tumor growth and prevent resistance or tumor recurrence by targeting both the proliferative tumor bulk and relatively quiescent state cells.

Contributors

Conception and design: XX Liu and YX Luo. Acquisition of data: XX Liu, SY Peng, GN Tang, GP Xu, YM Xie, MX Zhu, DC Shen and YY Huang. Analysis and interpretation of data: XX Liu, SY Peng, HC Yu and YX Luo. They have accessed and verified the underlying data. Study supervision: XL Wang, HC Yu, MH Huang, XX Liu and YX Luo. Drafting of the manuscript: XX Liu and YX Luo. All authors read and approved the final version of the manuscript. XX Liu, SY Peng and YX Luo have accessed and verified the data, and XX Liu was responsible for the decision to submit the manuscript.

Data sharing statement

All primary data in this study will be made available upon request to the corresponding authors for individuals with appropriate data-sharing agreements. UMI-mRNA sequencing data have been deposited in the National Center for Biotechnology Information Gene Expression Omnibus repository (GSE214537).

Declaration of interests

No potential conflict of interest was reported by the authors.

Acknowledgments

Support for these studies was provided by the National Natural Science Foundation of China (No. 82173067; No. 81972245; No. 82272965; No. 81902877; No. 31900505; No. 32100627), the Natural Science Foundation of Guangdong Province (No. 2022A1515012656; No. 2021A1515010639; No. 2021A1515010134), Science and Technology Program of Guangzhou (No. 202201011004), the "Five Five" Talent Team Construction Project of the Sixth Affiliated Hospital Of Sun Yat-Sen University (No. P20150227202010244; No.P20150227202010251), the Excellent Talent Training Project of the Sixth Affiliated Hospital Of Sun Yat-Sen University (No. R2021217202512965), the Scientific Research Project of the Sixth Affiliated Hospital Of Sun Yat-Sen University (No. 2022JBGS07), the Program of Introducing Talents of Discipline to Universities, and National Key Clinical Discipline (2012).

Appendix A. Supplementary data

Supplementary data related to this article can be found at <https://doi.org/10.1016/j.ebiom.2023.104496>.

References

- Nencioni A, Caffa I, Cortellino S, Longo VD. Fasting and cancer: molecular mechanisms and clinical application. *Nat Rev Cancer*. 2018;18(11):707–719.
- Ajona D, Ortiz-Espinosa S, Lozano T, et al. Short-term starvation reduces IGF-1 levels to sensitize lung tumors to PD-1 immune checkpoint blockade. *Nat Cancer*. 2020;1(1):75–85.
- Lien EC, Vander Heiden MG. A framework for examining how diet impacts tumour metabolism. *Nat Rev Cancer*. 2019;19(11):651–661.
- Caffa I, Spagnolo V, Vernieri C, et al. Fasting-mimicking diet and hormone therapy induce breast cancer regression. *Nature*. 2020;583(7817):620–624.
- Lee C, Raffaghello L, Brandhorst S, et al. Fasting cycles retard growth of tumors and sensitize a range of cancer cell types to chemotherapy. *Sci Transl Med*. 2012;4(124):124ra27.
- Raffaghello L, Lee C, Safdie FM, et al. Starvation-dependent differential stress resistance protects normal but not cancer cells against high-dose chemotherapy. *Proc Natl Acad Sci U S A*. 2008;105(24):8215–8220.
- Pietrocola F, Pol J, Vacchelli E, et al. Caloric restriction mimetics enhance anticancer immunosurveillance. *Cancer Cell*. 2016;30(1):147–160.
- Turbitt WJ, Demark-Wahnefried W, Peterson CM, Norian LA. Targeting glucose metabolism to enhance immunotherapy: emerging evidence on intermittent fasting and calorie restriction mimetics. *Front Immunol*. 2019;10:1402.
- Dai X, Bu X, Gao Y, et al. Energy status dictates PD-L1 protein abundance and anti-tumor immunity to enable checkpoint blockade. *Mol Cell*. 2021;81(11):2317–2331.e6.
- Siegel RL, Miller KD, Fuchs HE, Jemal A. Cancer statistics, 2021. *CA A Cancer J Clin*. 2021;71(1):7–33.
- Chen S, Zhang L, Li M, et al. Fusobacterium nucleatum reduces METTL3-mediated m(6)A modification and contributes to colorectal cancer metastasis. *Nat Commun*. 2022;13(1):1248.
- Fang L, Yang Z, Zhang M, Meng M, Feng J, Chen C. Clinical characteristics and survival analysis of colorectal cancer in China: a retrospective cohort study with 13,328 patients from southern China. *Gastroenterol Rep (Oxf)*. 2021;9(6):571–582.
- Taylor SR, Falcone JN, Cantley LC, Goncalves MD. Developing dietary interventions as therapy for cancer. *Nat Rev Cancer*. 2022;22(8):452–466.
- Smith CA, Want EJ, O'Maille G, Abagyan R, Siuzdak G. XCMS: processing mass spectrometry data for metabolite profiling using nonlinear peak alignment, matching, and identification. *Anal Chem*. 2006;78(3):779–787.
- Weng ML, Chen WK, Chen XY, et al. Fasting inhibits aerobic glycolysis and proliferation in colorectal cancer via the Fdft1-mediated AKT/mTOR/HIF1 α pathway suppression. *Nat Commun*. 2020;11(1):1869.
- Di Tano M, Raucci F, Vernieri C, et al. Synergistic effect of fasting-mimicking diet and vitamin C against KRAS mutated cancers. *Nat Commun*. 2020;11(1):2332.
- de Gramont A, Figer A, Seymour M, et al. Leucovorin and fluorouracil with or without oxaliplatin as first-line treatment in advanced colorectal cancer. *J Clin Oncol*. 2000;18(16):2938–2947.

- 18 D'Aronzo M, Vinciguerra M, Mazza T, et al. Fasting cycles potentiate the efficacy of gemcitabine treatment in vitro and in vivo pancreatic cancer models. *Oncotarget*. 2015;6(21):18545–18557.
- 19 Xu K, Wang R, Xie H, et al. Single-cell RNA sequencing reveals cell heterogeneity and transcriptome profile of breast cancer lymph node metastasis. *Oncogenesis*. 2021;10(10):66.
- 20 Baldominos P, Barbera-Mourelle A, Barreiro O, et al. Quiescent cancer cells resist T cell attack by forming an immunosuppressive niche. *Cell*. 2022;185(10):1694–1708.e19.
- 21 Lu H, Chen I, Shimoda LA, et al. Chemotherapy-induced Ca(2+) release stimulates breast cancer stem cell enrichment. *Cell Rep*. 2017;18(8):1946–1957.
- 22 Kobayashi Y, Masuda T, Fujii A, et al. Mitotic checkpoint regulator RAE1 promotes tumor growth in colorectal cancer. *Cancer Sci*. 2021;112(8):3173–3189.
- 23 Hinohara K, Wu HJ, Vigneau S, et al. KDM5 histone demethylase activity links cellular transcriptomic heterogeneity to therapeutic resistance. *Cancer Cell*. 2018;34(6):939–953.e9.
- 24 Han Y, Cai H, Ma L, et al. Nuclear orphan receptor NR4A2 confers chemoresistance and predicts unfavorable prognosis of colorectal carcinoma patients who received postoperative chemotherapy. *Eur J Cancer*. 2013;49(16):3420–3430.
- 25 Bulut-Karslioglu A, Biechele S, Jin H, et al. Inhibition of mTOR induces a paused pluripotent state. *Nature*. 2016;540(7631):119–123.
- 26 Rehman SK, Haynes J, Collignon E, et al. Colorectal cancer cells enter a diapause-like DTP state to survive chemotherapy. *Cell*. 2021;184(1):226–242.e21.
- 27 de Groot S, Lugtenberg RT, Cohen D, et al. Fasting mimicking diet as an adjunct to neoadjuvant chemotherapy for breast cancer in the multicentre randomized phase 2 DIRECT trial. *Nat Commun*. 2020;11(1):3083.
- 28 Brown JA, Yonekubo Y, Hanson N, et al. TGF- β -Induced quiescence mediates chemoresistance of tumor-propagating cells in squamous cell carcinoma. *Cell Stem Cell*. 2017;21(5):650–664.e8.
- 29 Hangauer MJ, Viswanathan VS, Ryan MJ, et al. Drug-tolerant persister cancer cells are vulnerable to GPX4 inhibition. *Nature*. 2017;551(7679):247–250.
- 30 Dixon SJ, Lemberg KM, Lamprecht MR, et al. Ferroptosis: an iron-dependent form of nonapoptotic cell death. *Cell*. 2012;149(5):1060–1072.
- 31 Liu Y, Zhou L, Xu Y, et al. Heat shock proteins and ferroptosis. *Front Cell Dev Biol*. 2022;10:864635.
- 32 Blomme A, Ford CA, Mui E, et al. 2,4-dienoyl-CoA reductase regulates lipid homeostasis in treatment-resistant prostate cancer. *Nat Commun*. 2020;11(1):2508.
- 33 Zhao C, Yu D, He Z, et al. Endoplasmic reticulum stress-mediated autophagy activation is involved in cadmium-induced ferroptosis of renal tubular epithelial cells. *Free Radic Biol Med*. 2021;175:236–248.
- 34 Mizushima N, Komatsu M. Autophagy: renovation of cells and tissues. *Cell*. 2011;147(4):728–741.
- 35 Byun S, Seok S, Kim YC, et al. Fasting-induced FGF21 signaling activates hepatic autophagy and lipid degradation via JMJD3 histone demethylase. *Nat Commun*. 2020;11(1):807.
- 36 Zhou B, Liu J, Kang R, Klionsky DJ, Kroemer G, Tang D. Ferroptosis is a type of autophagy-dependent cell death. *Semin Cancer Biol*. 2020;66:89–100.
- 37 Hou W, Xie Y, Song X, et al. Autophagy promotes ferroptosis by degradation of ferritin. *Autophagy*. 2016;12(8):1425–1428.
- 38 Huang T, Xu T, Wang Y, et al. Cannabidiol inhibits human glioma by induction of lethal mitophagy through activating TRPV4. *Autophagy*. 2021;17(11):3592–3606.
- 39 Kanarek N, Petrova B, Sabatini DM. Dietary modifications for enhanced cancer therapy. *Nature*. 2020;579(7800):507–517.
- 40 Mu E, Wang J, Chen L, Lin S, Chen J, Huang X. Ketogenic diet induces autophagy to alleviate bleomycin-induced pulmonary fibrosis in murine models. *Exp Lung Res*. 2021;47(1):26–36.
- 41 Lee C, Safdie FM, Raffaghello L, et al. Reduced levels of IGF-I mediate differential protection of normal and cancer cells in response to fasting and improve chemotherapeutic index. *Cancer Res*. 2010;70(4):1564–1572.
- 42 Di Biase S, Lee C, Brandhorst S, et al. Fasting-mimicking diet reduces HO-1 to promote T cell-mediated tumor cytotoxicity. *Cancer Cell*. 2016;30(1):136–146.
- 43 Vernieri C, Fucà G, Ligorio F, et al. Fasting-mimicking diet is safe and reshapes metabolism and antitumor immunity in patients with cancer. *Cancer Discov*. 2022;12(1):90–107.
- 44 Krstic J, Reinisch I, Schindlmaier K, et al. Fasting improves therapeutic response in hepatocellular carcinoma through p53-dependent metabolic synergism. *Sci Adv*. 2022;8(3):eabn2635.
- 45 Orlich MJ, Singh PN, Sabatè J, et al. Vegetarian dietary patterns and the risk of colorectal cancers. *JAMA Intern Med*. 2015;175(5):767–776.
- 46 Tabung FK, Liu L, Wang W, et al. Association of dietary inflammatory potential with colorectal cancer risk in men and women. *JAMA Oncol*. 2018;4(3):366–373.
- 47 Klurfeld DM, Weber MM, Kritchevsky D. Inhibition of chemically induced mammary and colon tumor promotion by caloric restriction in rats fed increased dietary fat. *Cancer Res*. 1987;47(11):2759–2762.
- 48 Prager BC, Xie Q, Bao S, Rich JN. Cancer stem cells: the architects of the tumor ecosystem. *Cell Stem Cell*. 2019;24(1):41–53.
- 49 Wu X, Wu MY, Jiang M, et al. TNF- α sensitizes chemotherapy and radiotherapy against breast cancer cells. *Cancer Cell Int*. 2017;17:13.
- 50 Kim BJ, Forbes NS. Single-cell analysis demonstrates how nutrient deprivation creates apoptotic and quiescent cell populations in tumor cylindroids. *Biotechnol Bioeng*. 2008;101(4):797–810.
- 51 Ahmed F, Haass NK. Microenvironment-driven dynamic heterogeneity and phenotypic plasticity as a mechanism of melanoma therapy resistance. *Front Oncol*. 2018;8:173.
- 52 Echeverria GV, Ge Z, Seth S, et al. Resistance to neoadjuvant chemotherapy in triple-negative breast cancer mediated by a reversible drug-tolerant state. *Sci Transl Med*. 2019;11(488).
- 53 Ebinger S, Özdemir EZ, Ziegenhain C, et al. Characterization of rare, dormant, and therapy-resistant cells in acute lymphoblastic leukemia. *Cancer Cell*. 2016;30(6):849–862.
- 54 Lawson MA, McDonald MM, Kovacic N, et al. Osteoclasts control reactivation of dormant myeloma cells by remodelling the endosteal niche. *Nat Commun*. 2015;6:8983.
- 55 Schürch C, Riether C, Amrein MA, Ochsenbein AF. Cytotoxic T cells induce proliferation of chronic myeloid leukemia stem cells by secreting interferon- γ . *J Exp Med*. 2013;210(3):605–621.
- 56 Recasens A, Munoz L. Targeting cancer cell dormancy. *Trends Pharmacol Sci*. 2019;40(2):128–141.
- 57 Phan TG, Croucher PI. The dormant cancer cell life cycle. *Nat Rev Cancer*. 2020;20(7):398–411.
- 58 Tang D, Chen X, Kang R, Kroemer G. Ferroptosis: molecular mechanisms and health implications. *Cell Res*. 2021;31(2):107–125.
- 59 Stockwell BR. Ferroptosis turns 10: emerging mechanisms, physiological functions, and therapeutic applications. *Cell*. 2022;185(14):2401–2421.
- 60 Gao M, Monian P, Pan Q, Zhang W, Xiang J, Jiang X. Ferroptosis is an autophagic cell death process. *Cell Res*. 2016;26(9):1021–1032.
- 61 Gregor A, Huber L, Auernigg-Haselmaier S, et al. A Comparison of the impact of restrictive diets on the gastrointestinal tract of mice. *Nutrients*. 2022;14(15).